JOURNAL OF GUIDANCE, CONTROL, AND DYNAMICS
Vol. 20, No. 6, November–December 1997

Momentum Transfer Dynamics of a Gyrostat with a Discrete Damper

Christopher D. Hall*
U.S. Air Force Institute of Technology, Wright–Patterson Air Force Base, Ohio 45433-7765

The stability of motion of attitude maneuvers of a torque-free rigid gyrostat with a discrete damper is investigated. The equations of motion are presented in dimensionless form. Conditions for equilibrium motions and for their stability are developed. Bifurcation diagrams are used to illustrate the stable and unstable branches of steady spins, and these bifurcation diagrams are interpreted in the slow state space of the rotor momenta and the unperturbed system Hamiltonian. The effect of the damper mechanism is illustrated using a perturbed version of the bifurcation diagram. A class of rotational maneuvers is developed based on maintaining a stationary-platform condition. This class of maneuvers maintains a small angular velocity, which has the effect of reducing the excitation of the flexible component.

Introduction

ASYMPTOTIC stability of steady spins of satellites depends on the effective use of energy dissipation to damp out motions caused by perturbing torques. It is also important to consider the effects of energy dissipation on the stability of motion during large-angle rotational maneuvers. A thorough investigation of the stability of steady spins of rigid bodies and of rigid gyrostats including energy sinks and discrete dampers was presented by Hughes.[1] A recent paper by Chang et al.[2] surveyed the types of damper mechanisms used in spacecraft. In an earlier paper, we obtained new results on the bifurcations that occur for a rigid body with a discrete damper in a principal plane and aligned parallel to the nominal spin axis.[3] The purpose of the present paper is to present the results of similar analyses of the motion of a rigid body containing flywheels that are used to absorb perturbing torques, i.e., reaction wheels, or to reorient the platform, i.e., momentum wheels. The motion of spacecraft with a single rotor has received much attention in the literature.[4,5] For multiple rotors, there are fewer results.[6,7] In this paper, we present the equations of a motion for an N-rotor gyrostat containing a discrete damper. The effect of the damper is investigated analytically for the case of a single-rotor gyrostat with aligned damper and rotor. A bifurcation diagram is used to illustrate the equilibrium motions in the case of no damper, and stability criteria are developed to characterize the effect of the damper. For multirotor gyrostats, a class of stationary-platform rotational maneuvers is developed based on maintaining a constant magnitude of the momentum wheel cluster. An example is used to illustrate the effectiveness of this type of maneuver in terms of reducing the motion of the flexible component of the spacecraft.

Model and Equations of Motion

The model studied (Fig. 1) comprises a rigid body $\mathcal{B}$ containing N rigid axisymmetric rotors $\mathcal{R}_j$ and a mass particle $\mathcal{P}$, which is constrained to move along a line $\boldsymbol{n}$ fixed in $\mathcal{B}$. The particle is connected to a linear spring and a linear dashpot damper. The reference axes $\boldsymbol{b}_i$ are fixed in the body. All vectors and tensors are expressed with respect to the body frame. This is a reasonable model for a spacecraft with momentum wheels and a ball-in-tube-type damper. It is also a reasonable model for approximating the motion of a spacecraft with a flexible appendage when only the first vibrational mode is important. In the former case, the mass of the particle would typically be a small fraction of the total mass, whereas in the latter case, the mass fraction may be more significant.

We neglect external forces and moments in developing the equations of motion, which are presented in dimensionless form. The superscript $*$ is used to denote dimensional quantities, and the nondimensionalization is presented subsequently. The linear and angular momentum of the system are denoted by $\boldsymbol{p}^*$ and $\boldsymbol{h}^*$, respectively. The linear momentum of the particle in the $\boldsymbol{n}$ direction is p_n^*, and the relative position and velocity of the particle in the $\boldsymbol{n}$ direction are x^* and y^*. The angular velocity of the body frame is $\boldsymbol{\omega}^*$, and the velocity of the point $\mathbf{O}$ is $\boldsymbol{v}_o^*$. The jth rotor $\mathcal{R}_j$ has axial direction $\boldsymbol{a}_j$, has angular momentum $h_{sj}^* = I_{sj}^* \omega_{sj}^*$ relative to the platform, and is subject to an axial torque g_{aj}^* applied by the platform. Collectively, the axial vectors are written as a $3 \times N$ matrix $\boldsymbol{A}$, the axial moments of inertia as an $N \times N$ diagonal matrix $\boldsymbol{I}_s$, the relative axial angular momenta as an $N \times 1$ matrix $\boldsymbol{h}_s^*$, and the axial torques as an $N \times 1$ matrix $\boldsymbol{g}_a^*$. The position vector from $\mathbf{O}$ to $\mathcal{P}$ is $\boldsymbol{r}_p^* = \boldsymbol{b}^* + x^* \boldsymbol{n}$, where $\boldsymbol{b}^*$ is a vector from the point $\mathbf{O}$ to the undeformed position of the particle. The mass of the particle is m_p^*, and the system mass is m^*. The first and second moments of inertia with respect to $\mathbf{O}$ are $\boldsymbol{c}^*$ and $\boldsymbol{I}^*$, and both depend on x^*. The symbol $\boldsymbol{I}_o^*$ denotes the moment of inertia when the particle is in its nominal position ($x^* = 0$). The spring has stiffness k^*, and the dashpot damper has damping coefficient c_d^*.

To nondimensionalize, we note that the angular momentum $\boldsymbol{h}^*$ has constant magnitude h^*, which we assume is nonzero. We then scale the variables and parameters as follows:

$$\begin{aligned}
&\boldsymbol{p}^* = \left(h^* m^* b^* / I_c^*\right)\boldsymbol{p} \qquad \boldsymbol{v}_o^* = \left(h^* b^* / I_c^*\right)\boldsymbol{v}_o \qquad \boldsymbol{h}^* = h^* \boldsymbol{h} \\
&\boldsymbol{\omega}^* = \left(h^* / I_c^*\right)\boldsymbol{\omega} \qquad \boldsymbol{h}_a^* = h^* \boldsymbol{h}_a \qquad \boldsymbol{\omega}_s^* = \left(h^* / I_c^*\right)\boldsymbol{\omega}_s \\
&p_n^* = \left(h^* m^* b^* / I_c^*\right) p_n \qquad y^* = \left(h^* b^* / I_c^*\right) y \qquad (1) \\
&x^* = b^* x \qquad t^* = \left(I_c^* / h^*\right) t \qquad \boldsymbol{b}^* = b^* \boldsymbol{b} \\
&\boldsymbol{c}^* = m_p^* x^* \boldsymbol{n} \qquad \boldsymbol{I}^* = I_c^* \boldsymbol{I} \qquad \boldsymbol{I}_s^* = I_c^* \boldsymbol{I}_s
\end{aligned}$$

and we define four dimensionless parameters as

$$\begin{aligned}
&\varepsilon = m_p^* / m^* \qquad b = m^* b^{*2} / I_c^* \\
&c_d = c_d^* I_c^* / (m^* h^*) \qquad k = k^* I_c^{*2} / (m^* h^{*2})
\end{aligned} \qquad (2)$$

The equations of motion for the special case of a single rotor may be found in Ref. 1 (pp. 218, 219). Here we present a reduced-dimensional form of the equations for the more general case of N rotors. In the form presented in Ref. 1, this would be a system of $8 + N$ ordinary differential equations for $\boldsymbol{p}$, $\boldsymbol{h}$, $\boldsymbol{h}_a$, p_n, and x.

Presented as Paper 97-0107 at the AIAA 35th Aerospace Sciences Meeting, Reno, NV, Jan. 6–9, 1997; received Jan. 27, 1997; revision received July 24, 1997; accepted for publication July 28, 1997.

*Assistant Professor of Aerospace and Systems Engineering, Department of Aeronautics and Astronautics, AFIT/ENY; currently Assistant Professor, Department of Aerospace and Ocean Engineering, Virginia Polytechnic Institute and State University, Blacksburg, VA 24061. E-mail: chall@aoe.vt.edu. Senior Member AIAA.

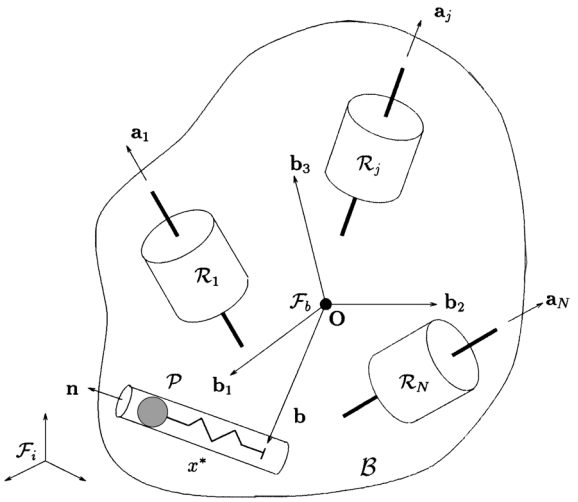

Fig. 1 *N*-rotor gyrostat with discrete damper.

Under the assumption of zero external force and moment, we can eliminate the linear momentum and the velocities, thereby reducing the equations to a system of $5 + N$ equations for $\boldsymbol{h}$, $\boldsymbol{h}_a$, p_n, and x,

$$\dot{\boldsymbol{h}} = \boldsymbol{h}^{\times}\boldsymbol{J}^{-1}\boldsymbol{m} \tag{3}$$

$$\dot{\boldsymbol{h}}_a = \boldsymbol{g}_a \tag{4}$$

$$\varepsilon \dot{p}_n = -\varepsilon c_d y - \varepsilon k x - \varepsilon^2 \boldsymbol{m}^T \boldsymbol{J}^{-1} \boldsymbol{n}^{\times} [(\varepsilon' x \boldsymbol{n} + \boldsymbol{b})^{\times} \boldsymbol{J}^{-1} \boldsymbol{m}] \tag{5}$$

$$\varepsilon \dot{x} = \varepsilon y \tag{6}$$

where $\varepsilon' = 1 - \varepsilon$, and

$$\boldsymbol{J} = \boldsymbol{I}_o - \boldsymbol{A}\boldsymbol{I}_s\boldsymbol{A}^T - \varepsilon\varepsilon' b x^2 \boldsymbol{n}^{\times}\boldsymbol{n}^{\times} + \varepsilon b[2x\boldsymbol{b}^T\boldsymbol{n}\mathbf{1} - x(\boldsymbol{b}\boldsymbol{n}^T + \boldsymbol{n}\boldsymbol{b}^T)] \tag{7}$$

$$\boldsymbol{m} = \boldsymbol{h} - \boldsymbol{A}\boldsymbol{h}_a - \varepsilon b y \boldsymbol{b}^{\times}\boldsymbol{n} \tag{8}$$

$$\varepsilon y = \frac{p_n + \varepsilon \boldsymbol{n}^T \boldsymbol{b}^{\times} \boldsymbol{J}^{-1} (\boldsymbol{h} - \boldsymbol{A}\boldsymbol{h}_a)}{\varepsilon' + \varepsilon b \boldsymbol{n}^T \boldsymbol{b}^{\times} \boldsymbol{J}^{-1} \boldsymbol{b}^{\times} \boldsymbol{n}} \tag{9}$$

The superscript $\times$ denotes the skew-symmetric matrix form of a vector.[1] Note that $\boldsymbol{J}^{-1}\boldsymbol{m} = \boldsymbol{\omega}$. These equations are in the form of singularly perturbed differential equations. When $\varepsilon = 0$, these equations reduce to the equations for a rigid N-rotor gyrostat (of dimension $3 + N$), for which Eq. (3) is a noncanonical Hamiltonian system.[5] The $\varepsilon = 0$ version of these equations has been investigated in Refs. 6 and 7.

Equilibrium Motions

There are several equilibrium solutions for Eqs. (3–6). Herein we restrict attention to equilibria for which the damper is motionless, i.e., x and $p_n = 0$. In this case, Eq. (6) implies $y = 0$. Thus from Eq. (9), either $\boldsymbol{\omega}$ is parallel to the $\boldsymbol{b}$ axis or $\boldsymbol{\omega}$ is in the plane spanned by $\boldsymbol{b}$ and $\boldsymbol{n}$ (assuming that $\boldsymbol{b}$ and $\boldsymbol{n}$ are not parallel). In addition, Eq. (3) implies that either $\boldsymbol{\omega} = \boldsymbol{0}$ or $\boldsymbol{\omega}$ is parallel to $\boldsymbol{h}$. The former condition is of particular interest because it is precisely the condition of a stationary platform, where all of the angular momentum is in the rotors. We will use this condition to investigate momentum transfer maneuvers that remain near this set of equilibria.

Momentum Transfer for Gyrostats

In Ref. 5 it was shown that, if the control torques $\boldsymbol{g}_a$ are small and constant, then the $N + 3$ equations of motion for a gyrostat may be reduced to a single first-order differential equation for the slow evolution of the Hamiltonian H. Furthermore, the $\boldsymbol{g}_a = \boldsymbol{0}$ branches of stable equilibria are integral curves of this averaged equation. Thus, the trajectories of constant-torque momentum transfer maneuvers that begin near a stable equilibrium (for $\boldsymbol{g}_a = \boldsymbol{0}$) will remain near the corresponding branch of stable equilibria unless the stability properties of that branch change, i.e., unless a bifurcation occurs. For $N \leq 2$, it is possible to interpret trajectories visually in the slow state space spanned by H and $\boldsymbol{h}_a$. In the following sections, we illustrate the slow state space for single-rotor gyrostats with discrete dampers. We also demonstrate the so-called stationary-platform maneuver for gyrostats with $N \geq 2$.

Axial Gyrostat with Aligned Damper

We consider the relatively simple case of a single-rotor, axial gyrostat with $N = 1$, with rotor axis $\boldsymbol{a} = \boldsymbol{b}_1$. We also align the damper parallel to the rotor spin axis ($\boldsymbol{n} = \boldsymbol{b}_1$) and align the vector $\boldsymbol{b}$ with the $\boldsymbol{b}_3$ axis. The simplification of the equations of motion is evident and is not repeated here (cf. Ref. 1, pp. 218–223).

For the calculations, the following parameters are used: $\boldsymbol{I} = \text{diag}(1.1, 0.8, 0.5)$, $I_s = 0.1$, $\varepsilon = 0.3$, and $c_d = 1$. Note that we have chosen $I_c^* = I_1^* - I_s^*$ so that $I_1' \triangleq I_1 - I_s = 1$. It is useful to define two inertia parameters by $i_2 = (J_1 - J_2)/(J_1 J_2)$ and $i_3 = (J_1 - J_3)/(J_1 J_3)$. For the inertias just given, $i_2 = 0.25$ and $i_3 = 1$.

Unperturbed and Perturbed Bifurcation Diagrams

For $\varepsilon = 0$, the momentum transfer dynamics of the axial gyrostat are well established.[4] The slow state space has been previously shown in Fig. 5 of Ref. 4, and equivalent information appears in Fig. 2. Note that this bifurcation diagram is symmetric about $h_a = 0$, so we focus our discussion on $h_a \geq 0$. Because Fig. 2 includes both the unperturbed ($\varepsilon = 0$) and perturbed ($\varepsilon \neq 0$) bifurcation diagrams, three different line styles and two different line thicknesses are used. Thin lines denote equilibria that exist in the unperturbed problem and do not exist in the perturbed problem. Thick lines denote equilibria that exist in both cases. Dashed lines denote unstable equilibria, solid lines denote stable equilibria, and the dot–dashed lines denote equilibria whose stability characteristics are determined by a relationship to be developed. Dotted lines indicate equilibria that are stable in the unperturbed problem but are destabilized by the damper mechanism.

The symbols O, P, T, and U in Fig. 2 denote oblate, prolate, transverse, and unstable, respectively, according to the type of equilibrium.[4] The oblate branch has positive momentum about the $\boldsymbol{b}_1$ axis [$\boldsymbol{h} = (1, 0, 0)$], whereas the prolate branch corresponds to a negative momentum about the $\boldsymbol{b}_1$ axis [$\boldsymbol{h} = (-1, 0, 0)$]. The transverse and unstable branches correspond roughly to spin about the $\boldsymbol{b}_2$ and $\boldsymbol{b}_3$ axes, but unless $h_a = 0$, these are not pure spins about these axes; rather there is a nonzero h_1 component. The bifurcations where T and U meet P are pitchforks and occur when $h_a = i_3$ and i_2, respectively. In summary, the O and T branches are stable, the P branch is stable for $0 \leq h_a < i_2$ and for $i_3 < h_a$, the P branch is unstable for $i_2 < h_a < i_3$, and the U branch is unstable.

When $\varepsilon \neq 0$, the U branch is changed and does not satisfy $x = 0 = p_n$ because any angular velocity about the $\boldsymbol{b}_2$ axis deflects the damper mass. The T branch is also changed and for $h_a \neq 0$ does not

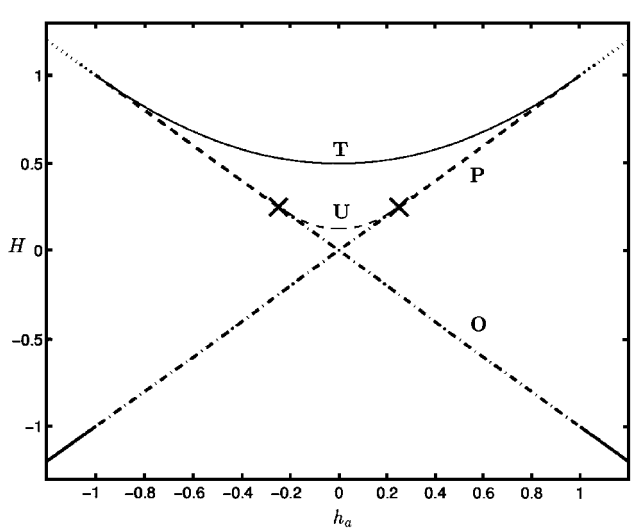

Fig. 2 Axial gyrostat, $h_a H$ plane.

satisfy $x = 0 = p_n$. Because we are only interested in the equilibria for which $x = 0 = p_n$, we do not compute the perturbed T and U branches here.

For this system, the most useful equilibria are the steady spins about the $\boldsymbol{b}_1$ axis, defined by $(\boldsymbol{h}, h_a, p_n, x)_e = (\pm 1, 0, 0, h_a, 0, 0)$, i.e., the O and P branches. The stability of these steady motions is of interest and clearly depends on the value of h_a, as well as the system parameters. From the symmetry of the problem (as evident in Fig. 2), we need only consider the $h_{1e} = +1$ case. We develop the linearized stability conditions using the Routh–Hurwitz criteria (Ref. 1, Chap. 7 and Appendix A), which can be simplified to

$$I_1' > -\max(I_2, I_3)\lambda \tag{10}$$

$$k > -\frac{\varepsilon^2 b \lambda^3}{I_1'^2 (I_1' + I_3 \lambda)} \tag{11}$$

where $\lambda = h_a - 1$. The modification to the bifurcation diagram due to the first criterion is shown in Fig. 2; note that this does not take into account the spring stiffness. The first of the two bifurcation points along the P branch persists (marked with an $\times$), but past the first bifurcation, the P branch is unstable.

Some specific cases are of interest. When $\lambda = -1$ ($h_a = 0$), it is straightforward to show that these are the familiar criteria for the spinning rigid body with a damper parallel to the spin axis.[3] When $\lambda = 0$, i.e., when all of the angular momentum is in the rotor, then stability is guaranteed because all of the stability conditions are met. When $\lambda > 0$, stability is also guaranteed.

When the first condition is not met, the equilibrium is unstable and no choice of damper parameters can stabilize the motion. This means that there is a critical value of $\lambda < 0$, denoted $\lambda^* = -I_1'/\max(I_2, I_3)$, that should not be within the operating range of the satellite. [Another way to put this is that $h_a > -\min(i_2, i_3)$ must be satisfied.] As a design consideration, then, it is appropriate to take

$$k > -\frac{\varepsilon^2 b \lambda^{*3}}{I_1'^2 \left(I_1' + I_3 \lambda^*\right)} \tag{12}$$

With Eq. (12) satisfied, the conditionally stable (dot–dashed lines) branches in Fig. 2 are asymptotically stable.

Remark. The linear stability analysis is slightly complicated by the presence of a zero eigenvalue: the first row and column of the linearized matrix are both zero. Thus, the stability of the center manifold[8] must be addressed. Recall the first integral due to conservation of angular momentum, $h^2 = 1$. At the O and P equilibria, the value of this first integral is $h_1^2 = 1$. Because h_2, h_3, p_n, and x all approach 0 asymptotically when the inequalities of Eqs. (10) and (11) are satisfied (they are in the stable manifold), h_1 must approach ± 1 asymptotically to preserve the integral. If the initial conditions are sufficiently near $h_1 = +1$, then h_1 must approach $+1$. Thus, at least locally, linear asymptotic stability implies nonlinear asymptotic stability, but the equilibria are not necessarily globally stable. In particular, for small values of h_a, both the O and P branches are asymptotically stable. This is similar to the two asymptotically stable spins of a quasirigid body about the major axis.

Stationary-Platform Maneuver

In this section we develop the concept of stationary-platform maneuvers for multirotor gyrostats. This class of maneuvers was previously reported for two-rotor gyrostats in Ref. 6 and for N-rotor gyrostats in Ref. 7. In this section we give an abbreviated development of the control law used to perform stationary-platform maneuvers for three-rotor gyrostats and then apply this control to a three-rotor gyrostat with discrete damper.

In the preceding section, we showed that the stationary-platform equilibrium is asymptotically stable for all physically realizable system parameters, for the special case of the axial gyrostat with aligned damper [Eq. (11) with $\lambda = 0$]. Such explicit criteria have not been developed for the more general case of a multirotor gyrostat with arbitrarily aligned damper. In the present work, we numerically verify that the stationary-platform equilibria are asymptotically stable by computing the eigenvalues of the linearized system.

A necessary condition for a stationary platform is that the angular momentum in the rotors has the same magnitude as the total system angular momentum, whereas a sufficient condition is that the rotor momentum is equal to the total system angular momentum. Mathematically, these conditions may be written as $\boldsymbol{h}_a^T \boldsymbol{A}^T \boldsymbol{A} \boldsymbol{h}_a = 1$ and $\boldsymbol{h} = \boldsymbol{A}\boldsymbol{h}_a$, respectively. The essence of the stationary-platform maneuver is to drive the rotor speeds from the initial conditions to the desired final conditions while maintaining the necessary condition. Because the averaging results of Ref. 5 are based on the assumption of a small torque, we apply that assumption here. Specifically, we assume that the internal torques may be written as $\boldsymbol{g}_a = \epsilon \boldsymbol{\sigma}$, where $|\epsilon| \ll 1$ and the elements of $\boldsymbol{\sigma}$ are all $\mathcal{O}(1)$. Then, because the stationary-platform equilibria are all stable, the trajectories should remain near the branch of stationary-platform equilibria and, hence, $\boldsymbol{\omega}$ should remain small. The advantage of such a trajectory is that the small platform angular velocities are less likely to excite vibrations in flexible components.

The necessary condition defines an ellipsoid in the N-dimensional $\boldsymbol{h}_a$ space. The initial and desired final stationary-platform equilibria define two points on this ellipsoid. The torques $\boldsymbol{g}_a$ are chosen such that the condition on $\boldsymbol{h}_a$ is satisfied throughout the maneuver. It is easy to show that any $\boldsymbol{g}_a$ that is orthogonal to $\boldsymbol{A}^T \boldsymbol{A} \boldsymbol{h}_a$ will yield such a maneuver. Thus, the torque vector $\boldsymbol{g}_a = \epsilon \boldsymbol{\sigma}$ must lie in the tangent space of the ellipsoid. For the $N = 2$ case, the ellipsoid is a simple ellipse, and the trajectory in $\boldsymbol{h}_a$ space simply traces the ellipse. For the $N = 3$ case, there are infinitely many choices for the trajectory because there are infinitely many curves connecting any two points on the ellipsoid.

One choice would be to take a geodesic that connects the two points, but this leads to complicated calculations and usually the ellipsoid will be nearly spherical. Therefore, we choose a path that lies in the intersection of the ellipsoid with a plane passing through the origin and containing the initial and final values of $\boldsymbol{h}_a$, denoted $\boldsymbol{h}_{ao}$ and $\boldsymbol{h}_{af}$, respectively. The development proceeds as follows. Define a new reference frame in $\boldsymbol{h}_a$ space with base vectors

$$\boldsymbol{c}_1 = \frac{\boldsymbol{h}_{ao}}{\|\boldsymbol{h}_{ao}\|} \tag{13}$$

$$\boldsymbol{c}_2 = \boldsymbol{c}_3^{\times} \boldsymbol{c}_1 \tag{14}$$

$$\boldsymbol{c}_3 = \frac{\boldsymbol{h}_{ao}^{\times} \boldsymbol{h}_{af}}{\left\| \boldsymbol{h}_{ao}^{\times} \boldsymbol{h}_{af} \right\|} \tag{15}$$

Collect these column matrices into a 3×3 rotation matrix, $\boldsymbol{C} = [\boldsymbol{c}_1 \ \boldsymbol{c}_2 \ \boldsymbol{c}_3]$, and define a transformed rotor momentum vector $\boldsymbol{\nu}$ by $\boldsymbol{\nu} = \boldsymbol{C}^T \boldsymbol{h}_a$. Under this transformation, the stationary-platform condition becomes $\boldsymbol{\nu}^T \boldsymbol{D}^T \boldsymbol{D} \boldsymbol{\nu} = 1$, where $\boldsymbol{D} = \boldsymbol{A}\boldsymbol{C}$. The columns of $\boldsymbol{D}$, to be denoted $\boldsymbol{d}_j$, are not unit vectors, even though the columns of $\boldsymbol{A}$ are. This relationship defines the ellipsoid in terms of the components of $\boldsymbol{\nu}$, and it is evident that $\boldsymbol{\nu}_o$ and $\boldsymbol{\nu}_f$ lie in the $\nu_1 \nu_2$ plane. Thus, $\nu_3 \equiv 0$ for the chosen trajectory, and the condition simplifies to

$$[\nu_1 \quad \nu_2] \begin{bmatrix} d_1^2 & \boldsymbol{d}_1^T \boldsymbol{d}_2 \\ \boldsymbol{d}_1^T \boldsymbol{d}_2 & d_2^2 \end{bmatrix} \begin{bmatrix} \nu_1 \\ \nu_2 \end{bmatrix} = 1 \tag{16}$$

Now, for the trajectory to follow the ellipse defined by Eq. (16), it is sufficient to take

$$\begin{bmatrix} \dot{\nu}_1 \\ \dot{\nu}_2 \end{bmatrix} = \epsilon \begin{bmatrix} -\boldsymbol{d}_1^T \boldsymbol{d}_2 & -d_2^2 \\ d_1^2 & \boldsymbol{d}_1^T \boldsymbol{d}_2 \end{bmatrix} \begin{bmatrix} \nu_1 \\ \nu_2 \end{bmatrix} \tag{17}$$

or

$$\dot{\boldsymbol{\nu}} = \epsilon \begin{bmatrix} -\boldsymbol{d}_1^T \boldsymbol{d}_2 & -d_2^2 & 0 \\ d_1^2 & \boldsymbol{d}_1^T \boldsymbol{d}_2 & 0 \\ 0 & 0 & 0 \end{bmatrix} \boldsymbol{\nu} = \epsilon \boldsymbol{E} \boldsymbol{\nu} \tag{18}$$

It is evident that $\dot{\boldsymbol{\nu}}$ is orthogonal to $\boldsymbol{D}^T \boldsymbol{D} \boldsymbol{\nu}$, thus satisfying the conditions for a stationary-platform maneuver. Substituting $\boldsymbol{\nu} = \boldsymbol{C}^T \boldsymbol{h}_a$ into the control leads to the desired control law for the rotor torques

$$\dot{\boldsymbol{h}}_a = \epsilon \boldsymbol{C} \boldsymbol{E} \boldsymbol{C}^T \boldsymbol{h}_a \tag{19}$$

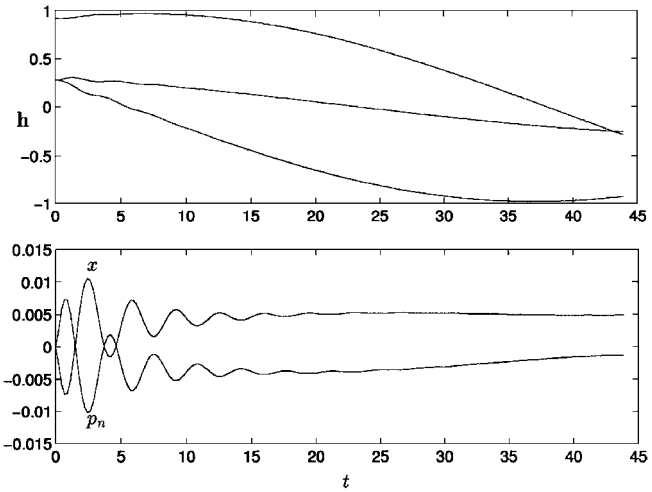

Fig. 3 Angular momentum and damper momentum and position for stationary-platform maneuver.

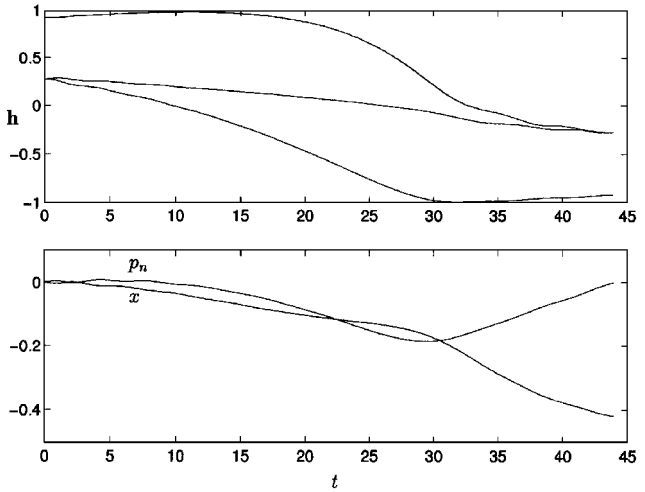

Fig. 4 Angular momentum and damper momentum and position for constant-torque maneuver.

This control law yields a stationary-platform maneuver. Because $\boldsymbol{C}$ and $\boldsymbol{E}$ are constant matrices depending only on $\boldsymbol{A}$ and the initial and final values of $\boldsymbol{h}_a$, this is a constant coefficient linear system of equations. Because $\boldsymbol{h}_a$ lies on the ellipsoid, it is evident that the torques are bounded and are $\mathcal{O}(\epsilon)$. Equation (19) can be solved in closed form and is decoupled from the platform dynamics. Thus, the stationary-platform maneuver is an easy-to-implement open-loop maneuver that is nearly optimal in two ways: the platform angular velocity is small throughout the maneuver and the motor torque is small throughout the maneuver because $\|\boldsymbol{g}_a\| = \mathcal{O}(\epsilon)$. It is also possible to view this control as a closed-loop control because $\boldsymbol{h}_a$ may be expressed in terms of the relative angular velocities of the rotors (as might be measured by tachometers) and the platform angular velocities (as might be measured by rate gyros).

For an example, we use the same parameters as for the preceding axial gyrostat example, with two additional rotors aligned with the $\boldsymbol{b}_2$ and $\boldsymbol{b}_3$ axes. The initial conditions are $\boldsymbol{h} = (0.9206, 0.2762, 0.2762)$, $\boldsymbol{h}_a = \boldsymbol{h}$, $p_n = 0$, and $x = 0$, and the desired final conditions are $\boldsymbol{h} = (-0.2762, -0.9206, -0.2762)$, $\boldsymbol{h}_a = \boldsymbol{h}$, $p_n = 0$, and $x = 0$. This corresponds to a maneuver through approximately 126 deg. Taking $\epsilon = 0.05$, the maneuver takes approximately 44 s. The angular momentum components and the particle momentum and position are shown in Fig. 3. The angular momentum reaches the desired final state, and the particle deflections are small.

For comparison, Fig. 4 shows the results of a constant torque maneuver from the initial to final values of rotor momentum. The torque magnitude is $\epsilon = 0.0293$, chosen so that the maneuver takes the same time as the stationary-platform maneuver. The trajectories in $\boldsymbol{h}$ space are similar, but the particle deflection is two orders of magnitude greater than in the stationary-platform case. For the constant torque maneuver, the angular velocity magnitude reaches ≈ 0.6 rad/s, whereas for the stationary-platform maneuver, the maximum angular velocity magnitude is ≈ 0.1 rad/s. Note that, if a pure eigenaxis rotation is used for this maneuver, the angular velocity would be about 0.035 rad/s and that the average value for the stationary-platform maneuver is about 0.051 rad/s. Thus, the stationary-platform maneuver is a simple approximation to an eigenaxis maneuver.

Conclusions

The combination of a discrete damper and a set of flywheels has significant effects on the motion of an otherwise rigid satellite. The system of equations describing the motion of such a satellite model is a perturbation of a noncanonical Hamiltonian system, and the underlying Hamiltonian structure is useful for understanding the dynamics. For the case of a single-rotor gyrostat with rotor and damper aligned with the major principal axis, it is possible to obtain explicit stability criteria that can be used in damper design or in the planning of momentum unloading operations. The Hamiltonian bifurcation diagram is an effective tool for interpretation of potential instabilities during attitude maneuvers. For multirotor gyrostats, explicit stability criteria are not available. Stationary-platform equilibria, however, appear to be asymptotically stable for all values of system parameters. This apparent fact leads to the usefulness of a class of attitude maneuvers based on steering the rotors along an ellipsoid defined by the stationary-platform condition. These stationary-platform maneuvers are significantly better than constant torque maneuvers in terms of angular velocity magnitude and the magnitude of excitation of the flexible component.

References

[1] Hughes, P. C., *Spacecraft Attitude Dynamics*, Wiley, New York, 1986, Chaps. 6 and 7.

[2] Chang, C. O., Liu, L. Z., and Alfriend, K. T., "Dynamics and Stability of a Freely Precessing Spacecraft Containing a Nutation Damper," *Journal of Guidance, Control, and Dynamics*, Vol. 19, No. 2, 1996, pp. 297–305.

[3] Chinnery, A. E., and Hall, C. D., "Motion of a Rigid Body with an Attached Spring-Mass Damper," *Journal of Guidance, Control, and Dynamics*, Vol. 18, No. 6, 1995, pp. 1404–1409.

[4] Hall, C. D., and Rand, R. H., "Spinup Dynamics of Axial Dual-Spin Spacecraft," *Journal of Guidance, Control, and Dynamics*, Vol. 17, No. 1, 1994, pp. 30–37.

[5] Hall, C. D., "Spinup Dynamics of Gyrostats," *Journal of Guidance, Control, and Dynamics*, Vol. 18, No. 5, 1995, pp. 1177–1183.

[6] Hall, C. D., "Momentum Transfer in Two-Rotor Gyrostats," *Journal of Guidance, Control, and Dynamics*, Vol. 19, No. 5, 1996, pp. 1157–1161.

[7] Hall, C. D., "Stationary-Platform Maneuvers of Gyrostat Satellites," *Dynamics and Control of Structures in Space III*, Computational Mechanics, Southampton, England, UK, 1996, pp. 337–348.

[8] Carr, J., *Applications of Center Manifold Theory*, Springer–Verlag, New York, 1981, pp. 1–29.